Preprints of the 21st IFAC World Congress (Virtual)
Berlin, Germany, July 12-17, 2020

Gait Generation for Underactuated Compass-Like Robots Using Dissipative Forces in the Controller ⋆

Matías Nacusse * **Pierluigi Arpenti** ** **Fabio Ruggiero** **
Vincenzo Lippiello **

* *Laboratorio de Automatización y Control (LAC). Departamento de Control, FCEIA, Universidad Nacional de Rosario, Argentina. CONICET. (e-mail: nacusse@fceia.unr.edu.ar)*
** *PRISMA Lab, Department of Electrical Engineering and Information Technology, University of Naples Federico II, Via Claudio 21, Naples, 80125, Italy (e-mail: {pierluigi.arpenti,fabio.ruggiero,vincenzo.lippiello}@unina.it)*

Abstract: This work addresses the problem of gait generation in underactuated compass-like biped robots using dissipative forces in the controller. Three different controllers are presented. The first one is a simultaneous interconnection and damping assignment passivity-based control with dissipative forces. The second one is an energy pumping-and-damping control, while the third one is an energy pumping or damping control action. Numerical case studies, comparisons, and critical discussions evaluate the performance of the proposed approaches.

Keywords: gait generation, compass-like robot, SIDA-PBC, pumping and damping, dissipative forces.

1. INTRODUCTION

A passive walker is a biped robot that exhibits a free and stable gait walking down a moderate slope under the effect of the gravitational field only. Its motion is referred to as *passive dynamic walking* and its gait as *passive gait*. The pioneering study of McGeer (1990) shows that such a particular kind of walking behavior occurs if the mechanical energy of the robot is constant during every single step. This is true due to the dissipation of the kinetic energy and the subsequent potential energy restoration supposing perfectly inelastic impacts between the biped's foot and the ground.

The focus on passive dynamic walking is mainly due to some physical similarities with the human walking and its energy efficiency. A particular kind of passive walker, the compass-like biped robot (***CBR***), synthesizes such a connection. The CBR, despite the simplest robotic kinematic structure compared to a human-like walking behavior, exhibits very complicated dynamics due to the hybrid nature of the system, as investigated by Goswami et al. (1996). A suitable way to control such kind of robot, exploiting its natural passive motion, is to adopt a passivity-based approach. Starting from a Lagrangian modeling framework, Spong and Bullo (2002) made the biped's gait invariant to slope changes via a potential energy shaping control based on the controlled-Lagrangian (***CL***) framework. The regulation of the biped's forward walking speed was achieved by Spong et al. (2007) with a potential energy shaping control too, successively extended with a total energy shaping approach with the goal to make the gait more robust over uncertainties on the initial conditions. A fully actuated biped robot model was considered by Spong and Bullo (2002) and Spong et al. (2007), while an underactuated compass-like biped robot (***UCBR***) was considered by Holm and Spong (2008), showing the effectiveness of a kinetic energy shaping approach to generate new gaits. These last were characterized by quick and long steps with satisfying robustness to uncertainties on the initial conditions. On the other hand, a gait with slow and short steps was obtained by De-León-Gómez et al. (2017) applying a control strategy based on the interconnection and damping assignment passivity-based control (***IDA-PBC***), rooted within the port-Hamiltonian (***pH***) framework and introduced by Ortega et al. (2001) and Ortega et al. (2002b). Arpenti et al. (2020) proposed a further IDA-PBC approach to generate both quick and long steps as well as slows and short ones.

The previous energy-based control methods define the closed-loop system, called the target system, in terms of the desired closed-loop energy function, interconnection, and dissipation structure. The pairing between the open-loop and the closed-loop system results in the so-called matching equations (MEs), which are partial differential equations (PDEs). The control input must satisfy the PDEs, which are the main bottleneck of these methodologies. Donaire et al. (2016) and Crasta et al. (2015) provide a survey review about solving the MEs. The IDA-PBC methodology, as shown by Ortega et al. (2002a), is carried out in two steps. The first one shapes the closed-loop energy, assigns the equilibrium point of the closed-loop system, and defines a possible new interconnection structure. The second step adds damping to ensure asymptotic stability. Some systems, as the induction machine, can not be solved using the two steps methodology of the IDA-PBC, requiring the *simultaneous* solution of the two steps methodology, as first

⋆ The research leading to these results has been partially supported by the WELDON project, in the frame of Programme STAR, financially supported by UniNA and Compagnia di San Paolo, and the PRINBOT project, in the frame of the PRIN 2017 research program with grant number 20172HHNK5_002.
Matías Nacusse thanks the SeCyT-UNR (Secretary for Science and Technology of the National University of Rosario) for the financial support through project PID-UNR 1ING502, and the ANPCyT (Argentine National Agency for Scientific and Technological Promotion), under project PICT 2017-3644.
The authors are solely responsible for its content.

done by Batlle et al. (2009). This results in the method called simultaneous IDA-PBC (***SIDA-PBC***).

As seen in the first part of this introduction, the restoration of mechanical energy is possible thanks to the (impulsive) dissipation, playing a leading role in such a physical phenomenon. Therefore, it seems natural to include dissipative forces inside the control action, aiming at creating new gaits. Donaire et al. (2016) extended the results of the SIDA-PBC method applied by Batlle et al. (2009) by introducing dissipative forces. They showed that several controllers for mechanical systems, designed without satisfying the two steps procedure of the standard IDA-PBC, fall under this new class of SIDA-PBC. Another control methodology which exploits dissipative forces is the energy pumping-and-damping control (***EPD***), which results in a slight modification of the standard damping injection term of the IDA-PBC. Such an EPD methodology was firstly introduced by Astrom et al. (2008) to stabilize an equilibrium point of a mechanical system, and by Yi et al. (2020) to generate stable orbits.

The main novelties of this work are twofold: the application of the SIDA-PBC with dissipative forces and the application of the EPD control to generate gaits in a UCBR. To the best of the authors' knowledge, these methodologies were never used to such a purpose. Besides, a particularization of the EPD methodology, which will be referred to as energy pumping or damping (***EPOD***) control, is also introduced in this paper as a further novelty to highlight the usefulness of dissipative forces for the generation of new UCBR gaits.

The organization of the paper is as follows. Section 2 presents a brief review of the SIDA-PBC methodology, the IDA-PBC with the pumping-and-damping term, and the EPOD control. Section 3 introduces the UCBR dynamic model. In Section 4, the design of the proposed controllers is carried out. Section 5 presents the obtained numerical results with a comparison and a critical analysis. Finally, Section 6 presents the conclusion and future work.

2. CONTROLLERS BACKGROUND

In this section, a brief review of the SIDA-PBC method using dissipative forces, the EPD control, and the EPOD control are presented.

2.1 SIDA-PBC

In this controller, the target system remains a mechanical system, while the control law modifies i) the closed-loop inertia matrix that defines the kinetic energy; ii) the potential energy; iii) the interconnection and dissipation structure. Among other advantages as the physical interpretation of the closed-loop system, it allows the solution of the MEs algebraically. The reader must refer to Donaire et al. (2016) for further details about this methodology.

Consider the following open-loop pH system

$$\begin{bmatrix} \dot{q} \\ \dot{p} \end{bmatrix} = \begin{bmatrix} 0_{n\times n} & I_{n\times n} \\ -I_{n\times n} & 0_{n\times n} \end{bmatrix} \nabla H + \begin{bmatrix} 0_{n\times m} \\ G(q) \end{bmatrix} u, \tag{1}$$

where q, $p \in \mathbb{R}^n$ are the generalised position and momenta, respectively, while the matrix $G(q) \in \mathbb{R}^{n\times m}$ weights the control inputs $u \in \mathbb{R}^m$. If m is equal to n, then the system is called *fully-actuated*, whereas $m < n$ it is called *under-actuated*. The function $H : \mathbb{R}^n \times \mathbb{R}^n \to \mathbb{R}$

$$H(q,p) = \frac{1}{2} p^T M^{-1}(q) p + V(q), \tag{2}$$

is the total energy with $M \in \mathbb{R}^{n\times n}$ the symmetric and positive definite inertia matrix, $V : \mathbb{R}^n \to \mathbb{R}$ the potential energy, and ∇H stands for the gradient vector, i.e. $\nabla H = [\nabla_q H \ \nabla_p H]^T = [\partial H/\partial q \ \partial H/\partial p]^T$.

Consider the target closed-loop system defined as

$$\begin{bmatrix} \dot{q} \\ \dot{p} \end{bmatrix} = \begin{bmatrix} 0_{n\times n} & M^{-1}M_d \\ -M_d M^{-1} & 0_{n\times n} \end{bmatrix} \nabla H_d + \begin{bmatrix} 0 \\ C(q,p) \end{bmatrix}, \tag{3}$$

where the function $H_d : \mathbb{R}^n \times \mathbb{R}^n \to \mathbb{R}$, defined as

$$H_d(q,p) = \frac{1}{2} p^T M_d^{-1}(q) p + V_d(q), \tag{4}$$

is the desired total energy, with $M_d \in \mathbb{R}^{n\times n}$ the symmetric and positive definite desired inertia matrix, $V_d : \mathbb{R}^n \to \mathbb{R}$ the desired potential energy, and $C : \mathbb{R}^n \times \mathbb{R}^n \to \mathbb{R}^n$ a mapping to be defined. The dependency on q in M, M_d, V, V_d, G and C is omitted to shorten the notation.

The ME resulting from equating (1) and (3) is

$$\begin{aligned} -\frac{1}{2}\nabla_q \left(p^T M^{-1} p\right) - \nabla V + Gu = \\ M_d M^{-1} \left[\frac{1}{2}\nabla_q \left(p^T M_d^{-1} p\right) + \nabla V_d\right] + C. \end{aligned} \tag{5}$$

If $G(q)$ is full rank, both terms of (5) can be multiplied by the left annihilator of $G(q)$, noted as $G(q)^\perp$, i.e. $G(q)^\perp G(q) = 0$, to obtain the following u-independent PDE

$$\begin{aligned} G^\perp \left[\frac{1}{2}\nabla_q \left(p^T M^{-1} p\right) + \nabla V\right] \\ - G^\perp \left[M_d M^{-1} \left[\frac{1}{2}\nabla_q \left(p^T M_d^{-1} p\right) + \nabla V_d\right] + C\right] = 0. \end{aligned} \tag{6}$$

As proposed by Ortega et al. (2002a), the PDE (6) can be split into the following p-independent equation

$$G^\perp \left(\nabla V - M_d M^{-1} \nabla V_d\right) = 0, \tag{7}$$

that is the so-called potential energy PDE (PE-PDE) (7), and into the following p-dependent equation

$$G^\perp \left(\nabla_q \left(p^T M^{-1} p\right) - M_d M^{-1} \nabla_q \left(p^T M_d^{-1} p\right) + 2C\right) = 0, \tag{8}$$

that is the so-called kinetic energy PDE (KE-PDE) (8). Since $C(q,0) = 0_n$, the related mapping can be expressed as

$$C(q,p) = \Lambda(q,p) M_d^{-1} p \tag{9}$$

for a matrix $\Lambda(q,p) \in \mathbb{R}^{n\times n}$ defined as

$$\Lambda := \begin{bmatrix} \Lambda_{11} & \Lambda_{12} \\ \Lambda_{21} & \Lambda_{22} \end{bmatrix}, \tag{10}$$

with Λ_{ij} some matrices of suitable dimensions. The mapping $C(q,p)$ must be quadratic in p and thus, without loss of generality, it can be written as

$$2C(q,p) = \sum_{i=1}^{n} \left(p^T M_d^{-1} Q_i M_d^{-1} p\right) e_i, \tag{11}$$

with $Q_i \in \mathbb{R}^{n\times n}$ free matrices to be chosen and $e_i \in \mathbb{R}^n$ the Euclidean basis vector.

Therefore, the desired closed-loop dynamics can be written as

$$\begin{bmatrix} \dot{q} \\ \dot{p} \end{bmatrix} = \begin{bmatrix} 0_{n\times n} & M^{-1}M_d \\ -M_d M^{-1} & \Lambda(q,p) \end{bmatrix} \nabla H_d. \tag{12}$$

A necessary condition for stability of the equilibrium point of the closed-loop system is $p^T M_d^{-1} \Lambda(q,p) M_d^{-1} p \leq 0$. Notice that this condition can be relaxed in this work since the main objective is not the regulation of the equilibrium point, but the gait generation. Once the MEs (7) and (8) are solved, then the control input can be algebraically computed as

$$u = \left(G^T G\right)^{-1} G^T \left[\nabla_q H - M_d M^{-1} \nabla_q H_d + \Lambda M_d^{-1} p\right]. \quad (13)$$

Notice that the dissipative forces in the controller are represented by the mapping C, as indicated by Donaire et al. (2016).

2.2 EPD control

Contrarily to the SIDA-PBC, within the IDA-PBC there exist two distinctive control actions, carried out separately in two consecutive steps. The former control action, u_{es}, is the so-called energy-shaping that shapes the closed-loop energy, assigns the desired equilibrium point of the closed-loop system, and defines a possible new interconnection structure. Such a control action results from the solution of (7) and (8) with the particular choice of $C = J_2 M_d^{-1} p$, where $J_2 \in \mathbb{R}^{n \times n}$ is a skew symmetric matrix. The latter control action, u_{di}, is the so-called damping-injection that adds damping to the actuated coordinates to ensure asymptotic stability, i.e. $u_{di} = -K_d G^T(q) \nabla_p H_d(q,p)$, where $K_d \in \mathbb{R}^{m \times m}$ is a positive semi-definite damping matrix to be tuned. The reader must refer to Ortega et al. (2002a) for a detailed description of the IDA-PBC regarding under-actuated mechanical systems, and the properties of the closed-loop system.

If the energy-shaping stage is ignored, i.e. $H_d(q,p) = H(q,p)$ and $J_2 = 0$, the IDA-PBC reduces to a controller which only dissipates the initial energy of the system. Then, the resulting control law comes out to be

$$u = -K_d G^T(q) \nabla_p H(q,p) = -K_d G^T(q) M^{-1}(q) p, \quad (14)$$

while the closed-loop system (1) becomes

$$\begin{bmatrix} \dot{q} \\ \dot{p} \end{bmatrix} = \begin{bmatrix} 0_{n \times n} & I_{n \times n} \\ -I_{n \times n} & R_d \end{bmatrix} \nabla H, \quad (15)$$

with $R_d = -G(q) K_d G^T(q)$, which asymptotically converges to its natural equilibrium, given that the passive output is detectable. Ortega et al. (2002b) and Van Der Schaft (2017) give additional insights about these aspects.

Remark. *Because the main objective of the controller is the gait generation, and not the asymptotic stabilization of an equilibrium point, the classical dissipation condition $R_d \leq 0$ can be relaxed. This implies that, in some regions of the state space, the R_d matrix is positive definite while, in other regions, it is negative definite. The same methodology was proposed by Astrom et al. (2008) to stabilize a pendulum in its upright position. Thanks to this modification, it is possible to refer to this controller as an EPD.*

The modification of the term (14) in an EPD controller leads to a control law u_{pd} with the following structure

$$u_{pd} = K_d f(q) G^T(q) M^{-1}(q) p, \quad (16)$$

with $f(q) : \mathbb{R}^n \to \mathbb{R}$ a suitable function such as

$$f(q) = \begin{cases} f_1(q) > 0 & \text{if } q \in S \\ f_2(q) \leq 0 & \text{if } q \in \mathbb{R}^n - S \end{cases} \quad (17)$$

where $S \subset \mathbb{R}^n$. Through such a control law, the time derivative of the total energy $H(q,p)$ becomes

$$\dot{H}(q,p) = p^T M^{-1}(q) G(q) K_d f(q) G^T(q) M^{-1}(q) p, \quad (18)$$

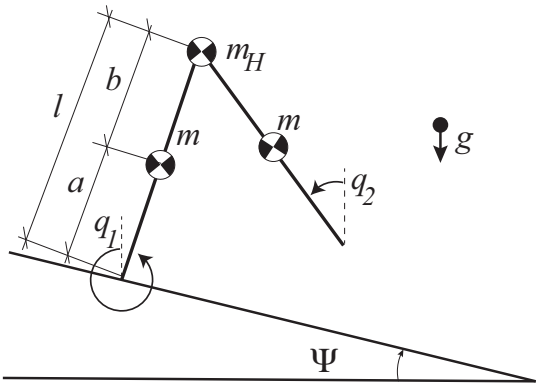

Fig. 1. Idealized physical system of the CBR.

whose sign changes accordingly with the sign of the function $f(q)$. The u_{pd} term, when $f(q)$ is such that $\dot{H}(q,p) \leq 0$, is a dissipative force.

2.3 EPOD control

The control methodology presented in the previous section can be slightly modified by designing a function $f(q)$ which is always positive. Albeit such a choice does not lead to an EPD controller, it brings to a control law that is different from the standard damping injection term of the IDA-PBC because of the dependency on the generalised coordinate vector introduced by $f(q)$. It is indeed equivalent to an energy damping controller, dissipating energy for $K_d < 0$. On the other hand, it reduces to an energy pumping controller for $K_d > 0$. The u_{pod} term assumes the role of a dissipative force for $K_d < 0$.

3. UCBR DYNAMIC MODEL

The CBR is a passive and planar walker exhibiting a stable symmetric gait under the gravity action only. Given a certain ground slope angle, $\psi > 0$, this is true whether both some geometric conditions are satisfied and the initial conditions are within the basin of attraction of the limit cycle representing the stable symmetric gait in the phase plane.

The idealized physical system of the CBR is shown in Fig. 1. The hip connects the two legs. For each step, the leg touching the ground is referred to as a *support leg*, while the swinging one is referred to as a *nonsupport leg*. The legs define two angles respect to the vertical gravity axis, called support and nonsupport angles, respectively. These two angles are referred to as q_1 and q_2, respectively, along with their velocities $\dot{q}_1$ and $\dot{q}_2$. The two angles and the related time-derivatives form the state space of the CBR. Despite the CBR is originally considered a fully actuated system, an UCBR is instead addressed in this work, following the approach pursued by Holm and Spong (2008) who put in the ankle of the support leg the primary actuation source relying on bio-mechanic arguments. The mathematical model describes the swing phase, that is the motion of the nonsupport leg before the impact with the ground. At each impact, the support and nonsupport legs are swapped.

Defining with $q = [q_1\ q_2]^T \in \mathbb{R}^2$ the vector of generalised coordinates, the inertia matrix of the UCBR is

$$M(q) = \begin{bmatrix} m_{11} & m_{12}\cos(q_1-q_2) \\ m_{12}\cos(q_1-q_2) & m_{22} \end{bmatrix} = \begin{bmatrix} (m_H+m)l^2+ma^2 & -mlb\cos(q_1-q_2) \\ -mlb\cos(q_1-q_2) & mb^2 \end{bmatrix}, \quad (19)$$

with $m_H > 0$ the hip mass, $m > 0$ the leg mass, $a > 0$ the distance between the foot and the leg mass, $b > 0$ the distance between the leg mass and the hip mass, and $l = a + b$. The UCBR has a potential energy

$$V(q) = (m(a+l)+m_H l)g\cos(q_1) - mbg\cos(q_2), \quad (20)$$

where $g > 0$ is the gravity acceleration. The pH mathematical model of the UCBR is thus defined as in (1), (2) with $G(q) = G = [1\ 0]^T$, inertia matrix (19), and potential energy (20). The swing phase is followed by the impact which occurs when

$$\begin{aligned} y_h(q) &= l[\cos(q_1+\psi) - cos(q_2+\psi)] = 0 \\ \dot{y}_h(q) &= l[\sin(q_2+\psi)\dot{q}_2 - sin(q_1+\psi)\dot{q}_1] < 0 \end{aligned} \quad (21)$$

where $y_h \in \mathbb{R}$ is the distance between the nonsupport leg's foot and the ground. An instantaneous change in the angular velocities is caused by the impact. With the assumption of a perfectly inelastic and non slipping contact between the nonsupport leg's foot and the ground, as well as an instantaneous transfer from supporting to nonsupporting one (no double-support phase admitted), such a change is described by the following equation

$$\dot{q}(t^+) = P(q(t^-))\dot{q}(t^-), \quad (22)$$

where $\dot{q} = [\dot{q}_1\ \dot{q}_2]^T$ is the velocity vector, while t^- and t^+ are the time instants just before and just after the impact, respectively. The matrix $P(q(t^-)) \in \mathbb{R}^{2\times 2}$, which is derived applying the law of conservation of angular momentum, has the following expression

$$P(q(t^-)) = \begin{bmatrix} p_{11}^+ & p_{12}^+ \\ p_{21}^+ & p_{22}^+ \end{bmatrix}^{-1} \begin{bmatrix} p_{11}^- & p_{12}^- \\ p_{21}^- & p_{22}^- \end{bmatrix}, \quad (23)$$

with $p_{11}^+ = ml(l - b\cos(q_1^- - q_2^-)) + ma^2 + m_H l^2$, $p_{12}^+ = mb(b - l\cos(q_1^- - q_2^-))$, $p_{21}^+ = -mbl(\cos(q_1^- - q_2^-))$, $p_{22}^+ = mb^2$, $p_{11}^- = -mab + (m_H l^2 + 2mal)\cos(q_1^- - q_2^-)$, $p_{12}^- = p_{21}^- = -mab$, $p_{22}^- = 0$. The reader can refer to the work of Goswami et al. (1996) for further details. Hence, the fully hybrid behavior of the UCBR is given by the composition of the swing and the impact phases. It is worth clarifying that it is not possible to physically realize such kind of robot due to the scuffing between the nonsupport leg's foot and the ground. Foot scuffing is avoided, in real prototypes, through specific mechanical designs, as, for instance, the one proposed by Bhounsule et al. (2012), making the UCBR worth of investigation anyhow. In this paper, foot scuffing is avoided by ignoring (21) whenever the nonsupport leg is behind the supporting one, as done by Holm and Spong (2008).

4. CONTROLLERS DESIGN

This section presents the design of the controllers. In the SIDA-PBC design subsection, a particular family of solutions is computed from the related MEs. First, the PE-PDE is solved by imposing that the closed-loop and the open-loop dependency to the potential energy with respect to q_2 are equal (i.e., $\nabla_{q_2} V = \nabla_{q_2} V_d$). Then, the KE-PDE is solved by fixing the structure of the Q_i matrices. Afterwards, in the EPD control design subsection, the function $f(q)$ appearing in (16) is computed. Finally, in the EPOD control design subsection, a change in such a function $f(q)$ is made.

4.1 SIDA-PBC design

Let

$$M_d(q) = \begin{pmatrix} m_{d_{11}}(q) & m_{d_{12}}(q) \\ m_{d_{12}}(q) & m_{d_{22}}(q) \end{pmatrix} \quad (24)$$

be the desired inertia matrix and

$$A := M_d M^{-1} = \begin{bmatrix} A_{11} & A_{12} \\ A_{21} & A_{22} \end{bmatrix} \quad (25)$$

the product between the desired inertia matrix and the inverse of the open loop one. Then, the PE-PDE (7) can be re-written as

$$G(q)^\perp \left(\begin{bmatrix} \nabla_{q_1} V \\ \nabla_{q_2} V \end{bmatrix} - A \begin{bmatrix} \nabla_{q_1} V_d \\ \nabla_{q_2} V_d \end{bmatrix} \right) = 0. \quad (26)$$

Taking into account that

$$G^\perp(q) = \begin{pmatrix} 0 \\ 1 \end{pmatrix}, \quad (27)$$

the PE-PDE (26) can be expressed as

$$\nabla_{q_2} V - A_{21}\nabla_{q_1} V_d - A_{22}\nabla_{q_2} V_d = 0. \quad (28)$$

The PDE (28) is solved choosing $A_{21} = 0$ and $A_{22} = 1$. Hence, $m_{d_{22}} = m_{22}$ and $m_{d_{12}} = m_{12}\cos(q_1 - q_2)$. This implies that $\nabla_{q_1} V_d$ is left free to be chosen.

In order to solve the KE-PDE, folding (27) into (8) yields

$$\nabla_{q_2}\left(p^T M^{-1} p\right) - \nabla_{q_2}\left(p^T M_d^{-1} p\right) + 2C_2 = 0. \quad (29)$$

By fixing the structure of the Q_2 matrix as

$$Q_2 := \begin{bmatrix} Q_{11} & Q_{12} \\ Q_{12} & Q_{22} \end{bmatrix}, \quad (30)$$

the component Λ_{22} can be written in terms of $\dot{q}_1$, for simplicity reasons, and $m_{d_{11}}$, which is the only free component of the desired inertia matrix $M_d(q)$ so far, as

$$\Lambda_{22} = \frac{m_{12} m_{22}\sin(q_1-q_2)\left(m_{11} - m_{d_{11}}(q)\right)}{2m_{12}^2\cos^2(q_1-q_2) - 2m_{22}m_{d_{11}}(q)}\dot{q}_1. \quad (31)$$

Setting $\Lambda_{12} = \Lambda_{21}$ and $\Lambda_{11} = \Lambda_{22}$, a family of solutions for the KE-PDE is obtained through an appropriate selection of $m_{d_{11}}$. By fixing the structure of the matrices Q_2 and Λ, then the mapping $C(q,p)$ is completely defined. Therefore, the matrix Q_1 is determined intrinsically. Notice that, due to the switching conditions (21), the equilibrium point of the closed-loop system will be never reached if a stable limit cycle is generated. This implies that the stability condition can be relaxed to generate gaits.

4.2 EPD control design

Similarly to the considerations made by Holm and Spong (2008) relying on bio-mechanic arguments, pumping energy at the beginning of each step while dissipating it at the end

$$\begin{aligned} &\dot{H}(q,p) > 0 \text{ for } \zeta < q_1 < \pi \\ &\dot{H}(q,p) = 0 \text{ for } q_1 = \zeta \\ &\dot{H}(q,p) < 0 \text{ for } -\zeta < q_1 < 0 \end{aligned} \quad (32)$$

seems to be an effective way to achieve larger step lengths and shorter step periods for the generated gait. The other way round

$$\begin{aligned} &\dot{H}(q,p) < 0 \text{ for } \zeta < q_1 < \pi \\ &\dot{H}(q,p) = 0 \text{ for } q_1 = \zeta \\ &\dot{H}(q,p) > 0 \text{ for } -\zeta < q_1 < 0 \end{aligned} \quad (33)$$

leads instead to shorter step lengths and greater step periods for the generated gait. The introduction of the offset $\zeta > 0$ in the transition between the pumping regime and the damping one (and vice-versa) is motivated by the intuition that feeding energy to the system in a wider region of the phase plane should lead to a faster gait as, equivalently, subtracting it should take to a slower one, if compared to a transition in $q_1 = 0$. Therefore, given (18), the controller u_{pd} which realises the sought behavior in (32) and (33) is

$$u_{pd} = k_d \sin(q_1) G^T M^{-1}(q) p, \tag{34}$$

where the function $f(q) = \sin(q_1)$ defines the sign of $\dot{H}(q,p)$ once that the gain $k_d \in \mathbb{R}$ is fixed.

4.3 EPOD control design

The choice $f(q) = |\sin(q_1)q_1|$ transforms the control action (34) into the following energy pumping or damping controller

$$u_{pod} = k_d |\sin(q_1) q_1| G^T M^{-1}(q) p. \tag{35}$$

The control law (35) is equivalent to a damping injection control law for $k_d < 0$, while it pumps energy for $k_d > 0$ in the sense that

$$\begin{array}{l} \dot{H}(q,p) < 0 \text{ for } k_d < 0 \text{ and } \forall\, q_1 \\ \dot{H}(q,p) = 0 \text{ for } q_1 = 0 \text{ and } \forall\, k_d \\ \dot{H}(q,p) > 0 \text{ for } k_d > 0 \text{ and } \forall\, q_1 \end{array} \tag{36}$$

where the time derivative of the total energy, obtained by substituting $f(q) = |\sin(q_1)q_1|$ into (18), is given by

$$\dot{H}(q,p) = k_d |\sin(q_1) q_1| \dot{q_1}^2. \tag{37}$$

5. NUMERICAL EVALUATION

5.1 Overview

In this section, numerical simulations are carried out to evaluate the performance of the proposed approaches. The simulations are performed on a standard personal computer, with 16 Gb of memory, in the MATLAB environment. The dynamic model of the UCBR (i.e., the pH model of (1) and (2) with inertia matrix (19) and potential energy (20)) is numerically simulated through the *ODE*45 routine of MATLAB with the event detection option active to evaluate the leg-ground hit. The designed controller is implemented at a discrete-time step of 0.01 s, while the simulations last 40 s.The employed parameters for the UCBR system are the same used by Holm and Spong (2008): $m_H = 10$ kg, $m = 5$ kg, $a = 0.5$ m, $b = 0.5$ m, $g = 9.8$ m/s^2, and $\psi = 3$ deg.

In the literature, see for example Goswami et al. (1996), Holm and Spong (2008) or De-León-Gómez et al. (2017), a *step* is defined as two consecutive foot-ground impacts. The gaits of the UCBR are then characterised by two parameters: the space covered on the inclined by each step, that is referred to as *step length* S, and its *duration* T. The provided plots are referred to as time histories, even though they represent the evolution of S and T for each step.

5.2 Case studies

Particular solutions of the controllers briefly revised in Section 2 are designed to generate different gaits.

Inherently to the SIDA-PBC methodology, the desired closed-loop potential energy is defined as

$$V_d(q) = (m(a+l) + m_H l) g \cos(q_1 + k_3 \psi) - mbg \cos(q_2), \tag{38}$$

while the selection of the $m_{d_{11}}(q)$ component is

$$m_{d_{11}}(q) = \frac{m_{11}^2 m_{22} - [m_{11} + k_2 \sin(q_1 - q_2)] m_{12}^2 \cos^2(q_1 - q_2)}{m_{11} m_{22} - m_{12}^2 \cos^2(q_1 - q_2) - m_{22} k_2 \sin(q_1 - q_2)}, \tag{39}$$

with k_2 a gain to be selected in order to meet the requirements of $M_d(q)$. Hence, Λ_{ii}, with $i = 1, 2$, yields to

$$\Lambda_{ii} = \frac{m_{12} m_{22} k_i \sin^2(q_1 - q_2)}{2\left(m_{11} m_{22} - m_{12}^2 \cos^2(q_1 - q_2)\right)} \dot{q}_1. \tag{40}$$

Notice that, although Λ_{ii} depends on the velocity $\dot{q}_1$, this is always negative during a gait, since the the support leg rotates always counter-clock wise (see Fig. 1). Therefore, the control law (13) contains three gains, namely k_1, k_2, k_3, which must be tuned properly. Notice that, with the particular selection, $k_1 = 0$, $k_2 = 0$, $k_3 = 0$, the passive gait is recovered. With the addressed UCBR, the passive gait is characterised by step length $S = 0.5347$ m and period $T = 0.7343$ s.

Relatively to the EPD methodology, the offset ζ has been experimentally tuned to $\frac{\pi}{24}$ rad. Such a choice leads to a controller which exhibits gaits which are comparable with the others presented in this work.

Six case studies will be analyzed in the following. They start with the same initial conditions

$$q_0 = [0.2187 \;\; -0.3234 \;\; -1.0918 \;\; -0.3772]^T,$$

and they are compared with the passive gait. All the gains are experimentally tuned. The former two case studies regard the SIDA-PBC; the third and the fourth case studies focus on the EPD controller; the latter two case studies implement the EPOD controller.

Case Study I: In this case study, the SIDA-PBC controller gains have been selected as $k_1 = -0.01, k_2 = -15, k_3 = 0.92$. The obtained gait has a very small step length $S = 0.1312$ m and a big time period $T = 0.8639$ s. The time histories of the gait step length S and the gait period T are depicted in Fig. 2.

Case Study II: In this case study, the SIDA-PBC controller gains have been selected as $k_1 = -0.15, k_2 = 0, k_3 = 0$. The obtained gait has a bigger step length, $S = 0.6084$ m, and a smaller time period, $T = 0.7144$ s, than the passive gait. The time histories of the step length S and the period T are depicted in Fig. 3. The comparison of the obtained limit cycles in the first two case studies with the passive gait is depicted in Fig. 4.

Case Study III: In this case study, the gain of the EPD controller are tuned to $k_d = -30$. The obtained gain has a smaller step length, $S = 0.4899$ m, and a bigger time period, $T = 0.7418$ s, than the passive gait. The time histories of the step length S and the period T are depicted in Fig. 5.

Case Study IV: In this case study, the gain of the EPD controller has been selected as $k_d = 30$. The obtained gain has a bigger step length, $S = 0.5831$ m, and a smaller time period, $T = 0.7227$ s, than the passive gait. The time histories of the step length S and the period T are depicted in Fig. 6. The comparison of the limit cycles obtained in the third and fourth case studies with the passive gait is depicted in Fig. 7.

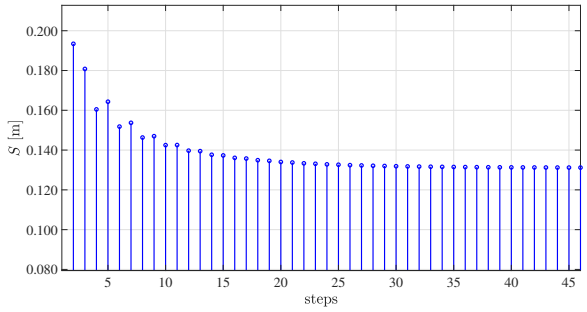

(a) Time history of S.

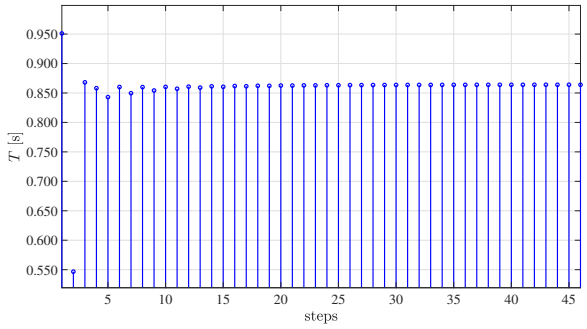

(b) Time history of T.

Fig. 2. Case Study I, SIDA-PBC, small gait obtained. Time histories of the step length and the step period during a test.

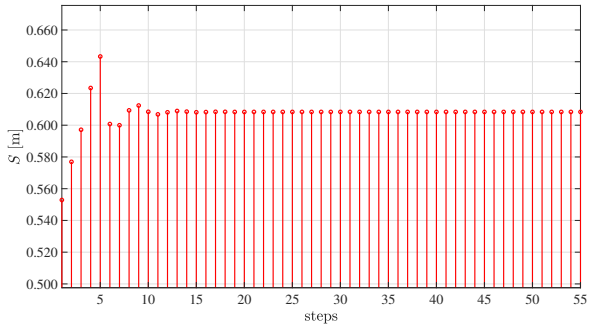

(a) Time history of S.

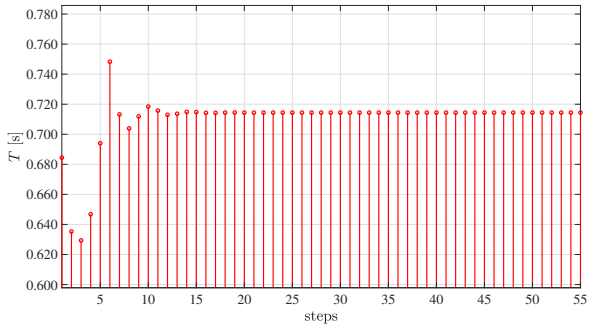

(b) Time history of T.

Fig. 3. Case Study II, SIDA-PBC, large gait obtained. Time histories of the step length and the step period during a test.

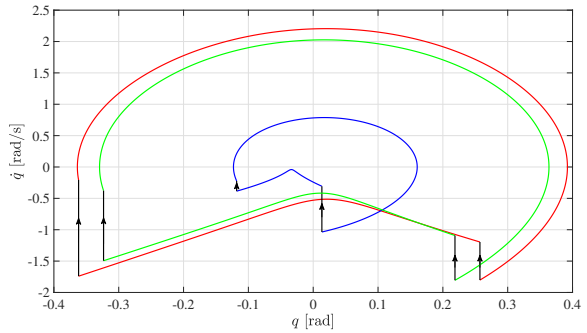

Fig. 4. Limit cycles comparison. In green, the passive gait. In blue, the Case Study I. In red, the Case Study II. In black, the discontinuities occurring at the impact. The arrows indicate the time evolution.

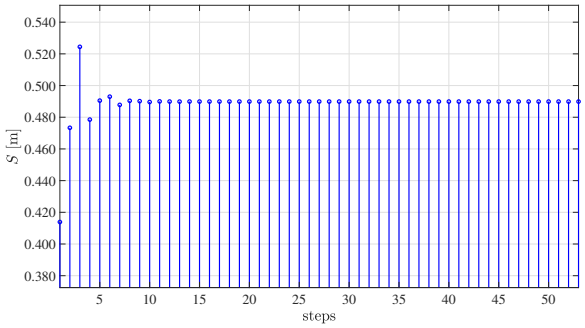

(a) Time history of S.

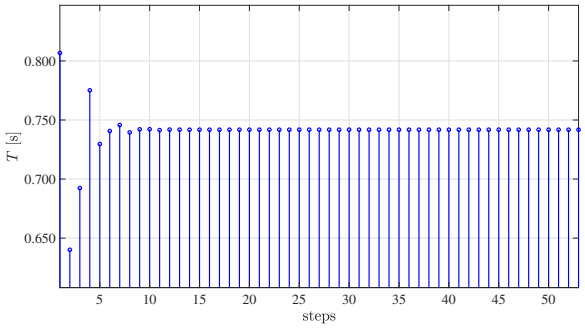

(b) Time history of T.

Fig. 5. Case Study III, EPD, small gait obtained. Time histories of the step length and the step period during a test.

Case Study V: In this case study, the gain of the EPOD controller has been tuned to $k_d = -280$. The obtained gait has a small step length $S = 0.4399$ m and a large time period $T = 0.7457$ s. The time histories of the step length S and the period T are depicted in Fig. 8.

Case Study VI: In this case study, the gain of the EPOD controller has been selected as $k_d = 160$. The obtained gait has a bigger step length, $S = 0.6394$ m, and a smaller time period, $T = 0.7286$ s, than the passive gait. The time histories of the step length S and the period T are depicted in Fig. 9. The limit cycles obtained in these two last examined case studies are compared with the passive gait within Fig. 10.

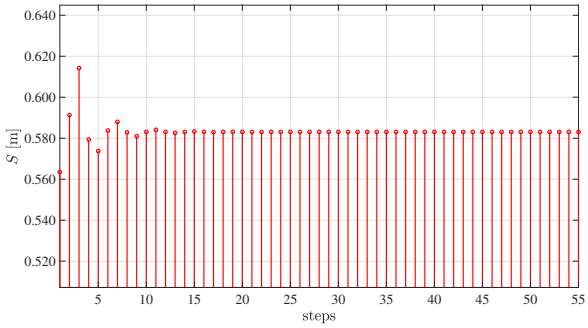

(a) Time history of S.

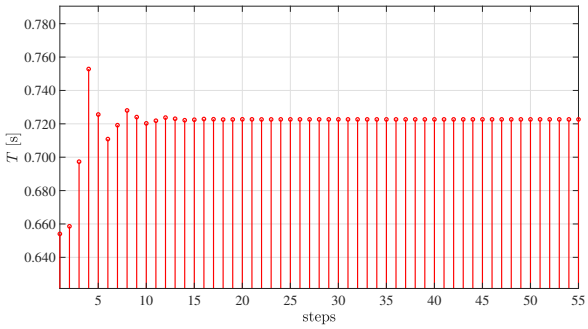

(b) Time history of T.

Fig. 6. Case Study IV, EPD, large gain obtained. Time histories of the step length and the step period during a test.

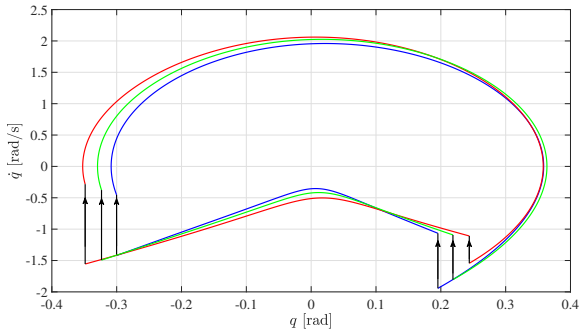

Fig. 7. Limit Cycles Comparison. In green, the passive gait. In blue, the Case Study III. In red, the Case Study IV. In black, the discontinuities occurring at the impact. The arrows indicate the time evolution.

5.3 Performance comparison

The comparisons depicted in Fig. 4, Fig. 7, and Fig. 10 between the limit cycles relative to all the case studies and the passive gait, as well as the time histories of the parameters S and T depicted in Fig. 3, Fig. 6, and Fig. 9, show that all the controllers are comparable with respect to the generation of larger gaits than the passive one. In particular, the EPOD can increase the step length of the passive gait of ≈ 0.1 m, versus the ≈ 0.07 m of the SIDA-PBC, and the ≈ 0.05 m of the EPD. The maximum period decreases of ≈ 2 s by employing the SIDA-PBC.

On the other hand, the blue limit cycles in Fig. 4, Fig. 7, and Fig. 10 show that SIDA-PBC is more effective in creating narrow limit cycles compared to the EPOD and the EPD. This is certified by the time histories in Fig. 2, Fig. 5, and Fig. 8 which

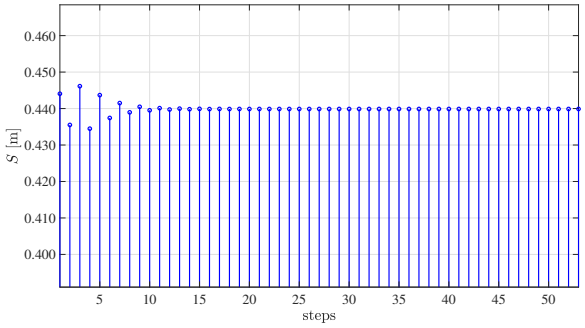

(a) Time history of S.

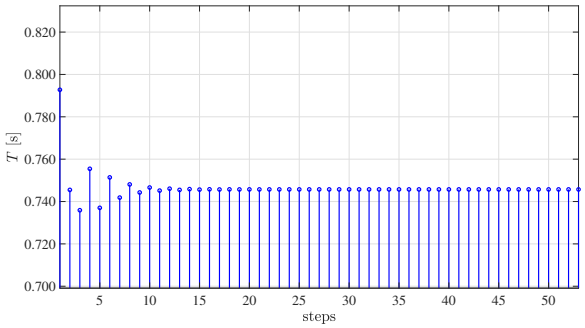

(b) Time history of T.

Fig. 8. Case Study V, EPOD, small gait obtained. Time histories of the step length and the step period during a test.

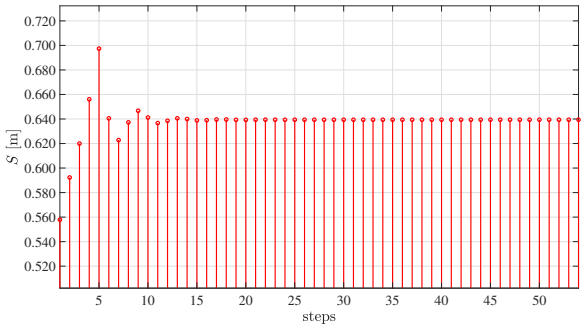

(a) Time history of S.

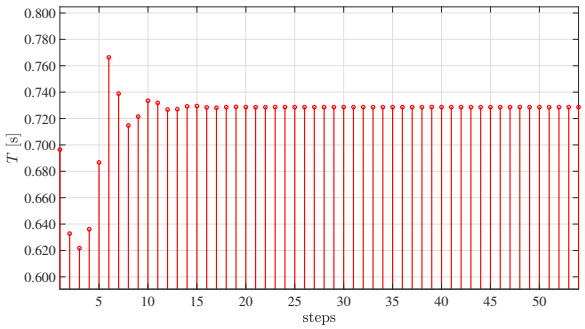

(b) Time history of T.

Fig. 9. Case Study VI, EPOD, large gait obtained. Time histories of the step length and the step period during a test.

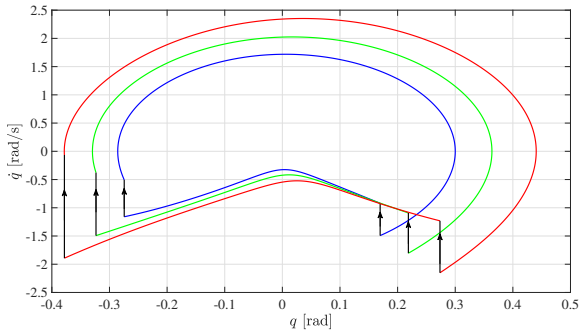

Fig. 10. Limit cycles comparison. In green, the passive gait. In blue, the Case Study V. In red, the Case Study VI. In black, the discontinuities occurring at the impact. The arrows indicate the time evolution.

show that the SIDA-PBC can produce stable gaits with the smallest step length, $S = 0.1312$ m, and the biggest time period, $T = 0.8639$ s, than the others. Besides, comparing the results of this work with those achieved by De-León-Gómez et al. (2017) who employed a standard IDA-PBC, emerges that the designed SIDA-PBC surpasses the IDA-PBC in the generation of small gaits. As a matter of fact, the smallest gait generated by De-León-Gómez et al. (2017) has $S = 0.2012$ m and $T = 0.9996$ s as parameters.

Therefore, the SIDA-PBC with dissipative forces seems to be the best choice if the sought goal is to generate gaits spreading from very small to large ones, especially if compared to other control strategies based on the exploitation of dissipative forces.

6. CONCLUSION AND FUTURE WORK

In this work, several control methodologies using dissipative forces, as the SIDA-PBC, the EPD control, and the EPOD control, were used to generate stable gaits for a UCBR. Due to the switching conditions produced by the impact of the swing leg with the ground, it was possible to generate a stable gait in a UCBR by relaxing the stability condition of the controllers mentioned above. In particular, it was possible to show that the SIDA-PBC, with the inclusion of dissipative forces, is efficient in the generation of gaits not exhibited by the uncontrolled system, especially compared to EPD and EPOD controllers. This might influence a more in-depth study about the applications of the SIDA-PBC for the gait generation problem. An idea is the research of a more significant set of solutions for the MEs. A further investigation of the relationship between gain tuning and the transient behavior of the UCBR might be carried out. Another possible future work is the formalization of the presented results to stabilize the gaits (i.e., the orbital stabilization problem), and not only to generate them. Finally, implementation on real hardware, with the proper adaptations to avoid foot scuffing, as mentioned at the end of Section 3, is undoubtedly a future scope.

REFERENCES

Arpenti, P., Ruggiero, F., and Lippiello, V. (2020). Interconnection and damping assignment passivity-based control for gait generation in underactuated compass-like robots. In *2020 IEEE International Conference on Robotics and Automation*. Paris, France.

Astrom, K.J., Aracil, J., and Gordillo, F. (2008). A family of smooth controllers for swinging up a pendulum. *Automatica*, 44(7), 1841–1848.

Batlle, C., Dòria-Cerezo, A., Espinosa-Pérez, G., and Ortega, R. (2009). Simultaneous interconnection and damping assignment passivity-based control: the induction machine case study. *International Journal of Control*, 82(2), 241–255.

Bhounsule, P., Cortell, J., and Ruina, A. (2012). Design and control of Ranger: An energy-efficient, dynamic walking robot. *Adaptive Mobile Robotics*, 441–448.

Crasta, N., Ortega, R., and Pillai, H.K. (2015). On the matching equations of energy shaping controllers for mechanical systems. *International Journal of Control*, 88(9), 1757–1765.

De-León-Gómez, V., Santibanéz, V., and Sandoval, J. (2017). Interconnection and damping assignment passivity-based control for a compass-like biped robot. *International Journal of Advanced Robotic Systems*, 14(4).

Donaire, A., Mehra, R., Ortega, R., Satpute, S., Romero, J.G., Kazi, F., and Singh, N.M. (2016). Shaping the energy of mechanical systems without solving partial differential equations. *IEEE Transactions on Automatic Control*, 61(4), 1051–1056.

Donaire, A., Ortega, R., and Romero, J. (2016). Simultaneous interconnection and damping assignment passivity-based control of mechanical systems using dissipative forces. *Systems & Control Letters*, 94, 118 – 126.

Goswami, A., Thuilot, B., and Espiau, B. (1996). Compass-like biped robot Part I: Stability and bifurcations of passive gaits. *Institut National de Recherche en Informatiqu et en Automatique (INRIA),Techical Report 2996*.

Holm, J. and Spong, M. (2008). Kinetic energy shaping for gait regulation of underactuated bipeds. In *IEEE International conference on control applications*, 1232–1238. San Antonio, Texas, USA.

McGeer, T. (1990). Passive dynamic walking. *International Journal of Robotic Research*, 9(2), 62–82.

Ortega, R., Spong, M., Gómez-Estern, F., and Blankenstein, G. (2002a). Stabilization of a class of underactuated mechanical systems via interconnection and damping assignment. *IEEE Transactions on Automatic Control*, 47(8), 1218–1233.

Ortega, R., Van Der Schaft, A., Mareels, I., and Maschke, B. (2001). Putting energy back into control. *IEEE Control Systems Magazine*, 18–33.

Ortega, R., Van Der Schaft, A., Maschke, B., and Escobar, G. (2002b). Interconnection and damping assignment passivity-based control of port-controlled Hamiltonian systems. *Automatica*, 38(4), 585–596.

Spong, M. and Bullo, F. (2002). Controlled symmetries and passive walking. In *Proceeding IFAC Triennal World Congress*. Barcelona, Spain.

Spong, M., Holm, J., and Lee, D. (2007). Passivity-based control of bipedal locomotion. *IEEE Robotics & Automation Magazine*, 12(2), 30–40.

Van Der Schaft, A. (2017). In *L_2-Gain and Passivity Techniques in Nonlinear Control*, Communications and Control Engineering. Springer, Berlin. ISBN 978-3-319-49991-8.

Yi, B., Ortega, R., Wu, D., and Zhang, W. (2020). Orbital stabilization of nonlinear systems via Mexican sombrero energy shaping and pumping-and-damping injection. *Automatica*, 112.